

Unpinning the Fermi level of GaN nanowires by ultraviolet radiation

Carsten Pfüller,* Oliver Brandt, Frank Grosse, Timur Flissikowski, Caroline Chèze, Vincent Consonni, Lutz Geelhaar, Holger T. Grahn, and Henning Riechert

Paul-Drude-Institut für Festkörperelektronik, Hausvogteiplatz 5-7, 10117 Berlin, Germany

(Received 26 May 2010; revised manuscript received 7 July 2010; published 29 July 2010)

We observe a significant increase in the photoluminescence intensity of GaN nanowires under continuous ultraviolet irradiation on a time scale of minutes. Experiments carried out under different ambient conditions demonstrate that this increase is caused by the photoinduced desorption of oxygen from the nanowire sidewalls. The slow, highly nonexponential temporal evolution of the photoluminescence signal is modeled by a random-walk approach. The model reveals that already desorbed oxygen molecules are likely to be readsorbed at adjacent nanowires. Time-resolved photoluminescence measurements are performed to unravel the correlation between the oxygen desorption and the increase in the photoluminescence intensity. We find that the oxygen desorption unpins the Fermi level, which in turn leads to an increase in quantum efficiency by enhancing the radiative decay of excitons.

DOI: [10.1103/PhysRevB.82.045320](https://doi.org/10.1103/PhysRevB.82.045320)

PACS number(s): 78.67.Uh, 68.43.Tj, 73.90.+f, 78.55.Cr

Semiconductor nanowires (NWs) are attracting a strongly increasing interest since they promise the integration of direct band gap (III/V or II/VI) semiconductors of high crystalline quality with Si.¹ They thus represent possible building blocks for nanometer-scale electronic and optoelectronic devices including field effect transistors, light sources, photodetectors,² and solar cells.³

On a more fundamental level, NWs have one distinguishing characteristic of utmost significance for these applications: their very large surface-to-volume ratio, which elevates the relevance of surface-related effects to a level not experienced in layers. For example, nonradiative surface recombination, which is hardly detectable for GaN layers, becomes important for GaN NWs.⁴ The transition energy of bound excitons in the vicinity of the surface is increased as described in our previous work.⁵ Self-purification⁶ enhances the tendency of both native point defects and impurities to assemble close to the NW surface. This segregation of point defects and impurities toward the surface⁷ boosts the electronic quality of NWs well beyond that of the corresponding bulk. However, it also interferes with the intentional and controlled doping of NWs due to surface depletion effects.⁸

The above examples do not only illustrate the importance of surface-related effects in NWs, but also demonstrate that an understanding of these effects is crucial for the successful application of NWs in nanometer-scale devices. Here, we present the observation of an unusual and very slow increase in photoluminescence (PL) intensity of as-grown GaN NW ensembles under continuous exposure to ultraviolet (UV) light. We show that this phenomenon is governed by a pure surface effect, namely, an unpinning of the surface Fermi level.

The investigated GaN NW sample has been grown by plasma-assisted molecular beam epitaxy (PAMBE) on a Si(111) substrate. The growth was performed under N-rich conditions at a substrate temperature of 780 °C, i.e., similar to the conditions reported by other groups.^{9,10} The detailed growth conditions can be found elsewhere.⁵ In general, the NW density is larger than 10^{10} cm⁻² with an average NW diameter of 40 nm. The average lengths of the NWs is about 400 nm. The temporal evolution of the PL signal has also

been studied for GaN layers from the same system as well as for several other GaN NW samples grown in a different MBE system.

Continuous-wave PL measurements have been performed at a temperature of 10 K in high vacuum [$(2-5) \times 10^{-6}$ mbar] after subjecting the samples to the *in situ* ozone cleaning described in Ref. 11. The 325 nm line of a HeCd laser with a maximum intensity of $I_0=20$ kW/cm² was focused by a $15 \times$ UV microscope objective with a numerical aperture of 0.32 to a spot of about 3 μ m diameter. The PL signal was then collected by the same objective and focused onto the entrance slit of an 80-cm spectrometer, which is equipped with a 600-lines/mm grating and an LN₂-cooled charge-coupled device array (CCD) for signal detection.

Time-resolved photoluminescence (TRPL) measurements were performed by exciting the NWs with the second harmonic of an optical parametric oscillator pumped by a femtosecond Ti:sapphire laser. The excitation wavelength was 325 nm with a pulse duration of 200 fs at a repetition rate of 76 MHz. The PL signal was dispersed by a 22-cm spectrometer and detected by a synchroscan streak camera. The system has a spectral resolution of 1 nm and a time resolution below 2 ps.

All PL and TRPL measurements were performed in back-scattering geometry. Note that the NW dimensions are in the subwavelength range, i.e., the wavelengths of both, the exciting as well as the emitted light, are larger than the NW diameter. Hence, regarding the coupling of light into a NW, wave optics rather than geometric optics has to be applied. Plane waves arriving at the NW ensemble will be diffracted at the NW tips. According to Huygens' principle each NW tip acts as point source for the generation of spherical waves that propagate in all directions. Thus, the NWs are actually excited over a length from the top that is typically larger than the absorption length, in particular due to the direct excitation through the NW sidewalls.

Figure 1(a) shows two near-band-gap PL spectra of the NW sample at the beginning (black solid line) and after 90 min (red dashed line) of continuous exposure to the UV laser with $10^{-5}I_0$. The donor-bound exciton (D^0, X) transition oc-

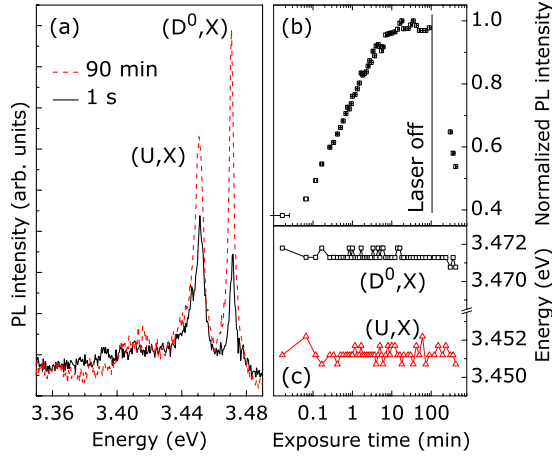


FIG. 1. (Color online) Evolution of the GaN NW PL signal under continuous UV exposure at 10 K and an excitation density of $10^{-5}I_0$. (a) PL spectra of the GaN NW ensemble after 1 s and 90 min of UV exposure. (b) Evolution of the spectrally integrated PL intensity. The UV laser has been turned off after 90 min of exposure to allow for readsorption. (c) Evolution of the peak energy of the (D^0,X) and (U,X) transition. Note the logarithmic scale of the time axis in (b) and (c).

occurs at 3.472 eV as expected for strain-free GaN.^{12–14} The line at 3.45 eV [labeled (U,X)] is characteristic for GaN NWs, but its origin has not yet been identified. Various possibilities have been debated, such as excitons bound to inversion domains or to abundant surface defects.^{5,9,15,16} In a recent publication,¹⁷ this line has been proposed to be the two-electron satellite (TES) of (D^0,X) complexes close to the surface. We will later on discuss the origin of this line in the light of our results. Finally, the band around 3.42 eV (which originates from stacking faults¹⁸) is excluded from further analysis because of its low intensity for this sample.

Most important, however, is the fact that the intensity of the (U,X) and, particularly, the (D^0,X) transitions increase drastically in these 90 min. We observe this effect with ongoing exposure to the UV laser regardless of sample temperature, but only as long as the NWs are kept in vacuum. Venting the cryostat with air instantaneously reverses this effect, while pure N_2 has no such effect. These results suggest that oxygen is responsible for the observed PL intensity evolution. Indeed, there have been reports on photoinduced oxygen desorption from the surface of GaN layers^{19,20} resulting in a PL intensity increase of up to 40%. The effect we observe, however, is much more significant, as shown exemplarily in Fig. 1(b). Depending on the experimental conditions such as temperature, excitation intensity, and the particular NW sample, we found the PL intensity to increase by a factor of 2 to 5. Note that the photodesorption of oxygen from the surface of semiconductors such as ZnO is a classical problem in surface chemistry and has been studied as early as the late 1950s.²¹ The desorption is induced by the transfer of photogenerated holes from the bulk to the surface, thus neutralizing negatively charged ionosorbed oxygen. In the case of NWs, the surface area is dominated by the NW sidewalls. As the whole NW volume is excited, the majority of

the photodesorbed oxygen originates from the sidewalls, while the contribution from the top facets is negligible.

Figure 1(b) displays the temporal evolution of the integrated PL signal (note the logarithmic time scale) under UV exposure. The laser was switched on at $t=0$ and off after 90 min of continuous illumination. Each PL spectrum has been recorded with an integration time of 1 s. The PL intensity increases in an essentially logarithmic manner and saturates after 10 min at about 260% of its initial value. All spectra after 90 min have been acquired under noncontinuous illumination, i.e., the NWs have been exposed to UV light only for the time needed to record a single spectrum, thus allowing for readsorption of oxygen (which has a partial pressure of 10^{-7} mbar) between the individual data points. The readsorption process is reflected by the slowly decreasing PL signal after the laser has been switched off.

Figure 1(c) shows that the spectral positions of both the (D^0,X) and the (U,X) transition do not change during the entire measurement. The increase in the PL intensity observed is thus not caused by a change of the recombination channel, but rather by an enhanced quantum efficiency.

The temporal behavior of the PL intensity in Fig. 1(b) reflects a highly nonexponential decay of the oxygen coverage of the NWs, which, at a first glance, seems not to be interpretable by standard first-order desorption kinetics. The most important aspect we have to consider for a quantitative understanding of this phenomenon is the specific geometry of the sample. Molecules which have been desorbed from NW a can be *readsorbed* at nearest-neighbor NWs $\{a\}$ with a probability $0 \leq \kappa \leq 1$, with $\kappa=0$ ($\kappa=1$) corresponding to no (complete) readsorption. When $\kappa > 0$, oxygen molecules will perform a *random walk* from NW to NW before leaving the NW ensemble irrevocably. Thus, the desorption process is prolonged for fundamental reasons. The value of the variable κ depends on the specific sample geometry, including NW density and distribution. In order to simplify modeling, we assume that the NWs are habitating an equidistant square lattice. As a consequence, κ is derived from an ensemble average and thus treated as a constant.

A certain fraction of the photogenerated holes will reach the NW sidewalls and contribute to the desorption process. Experimentally (see below), we find that this fraction varies with the excitation intensity I_L , i.e., the desorption rate Γ does *not* scale linearly with I_L . To account for this nonlinearity, we assume a power-law dependence of Γ on the excitation intensity with an exponent b . Note, that due to the Gaussian excitation profile $\gamma(\vec{r})$ the desorption rate is position dependent. This inherent spatial nonuniformity of Γ leads to a nonexponential decay of the oxygen coverage even for $\kappa=0$, i.e., in the case of layers.

The normalized oxygen coverage $0 \leq n_a(t) \leq 1$ of the a th NW at position \vec{r}_a is then described by

$$\frac{dn_a(t)}{dt} = -\Gamma_a n_a(t) + \kappa \frac{1 - n_a(t)}{4} \sum_{i=\{a\}} \Gamma_i n_i(t), \quad (1)$$

where the factor 1/4 accounts for the number of next neighbors. Initially, the oxygen coverage of the NWs is at its maximum, i.e., $n_a(t=0)$ is set to 1. The summation on the

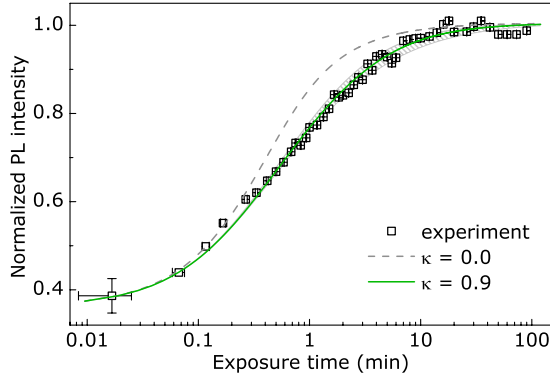


FIG. 2. (Color online) Evolution of the GaN NW PL signal under continuous UV exposure at 10 K and an excitation density of $10^{-5}I_0$. The experimental PL data of the GaN NW ensemble (symbols) are modeled with different readsorption probabilities κ . The gray shaded area depicts the range of high readsorption with $0.8 < \kappa < 1.0$.

right-hand side of Eq. (1) is restricted to the nearest neighbors $\{a\}$ of NW a . Simulations including additional coupling to next-nearest-neighbor NWs did not significantly affect our findings.

The PL intensity of the NW array can then be written as

$$I_{\text{PL}}(t) = I_{n=0} + I_{n=1} \sum_a n_a(t) \gamma(\vec{r}_a), \quad (2)$$

where $I_{n=0}$ is the intensity at the minimum oxygen coverage. The initial intensity is therefore $I_{\text{PL}}(t) = I_{n=0} + I_{n=1} \sum_a \gamma(\vec{r}_a)$ with $I_{n=1} \leq 0$ in the case of GaN.

The diameter of the excited area, the lattice spacing, and the PL intensities $I_{n=0}$ and $I_{n=1}$ as well as the excitation intensity I_L are taken from the experiment. The readsorption represented by κ and the exponent b are unknown parameters. b describes the acceleration of the desorption process with increasing excitation. In order to determine b , excitation dependent measurements have to be simulated. However, within the experimental error margin, b does not affect the shape of the simulated curve whose slope and curvature are thus primarily determined by κ . The present data set is best fitted by $\kappa=0.9$ (depicted by the green curve in Fig. 2). The comparison with different readsorption rates (which would be expected for samples with different NW densities) to the experimental data as shown in Fig. 2 demonstrates that, first of all, our observation is consistent with standard first-order desorption kinetics. Second, it shows that a significant amount of oxygen molecules is readsorbed on nearest-neighbor NWs and, thus, the desorption process is slowed down significantly.

One prediction of the model is that κ is independent of the laser power. We therefore performed room temperature desorption measurements for a second GaN NW sample at two different excitation densities as shown in Fig. 3 (blue squares $10^{-2}I_0$, red triangles $10^{-3}I_0$). Both data sets can be simulated consistently with $\kappa=0.75$. For the sample under investigation, the temporal shift between the two data sets corresponds to $b=0.34$. A more exhaustive analysis of the excitation dependence is hampered by experimental constraints.

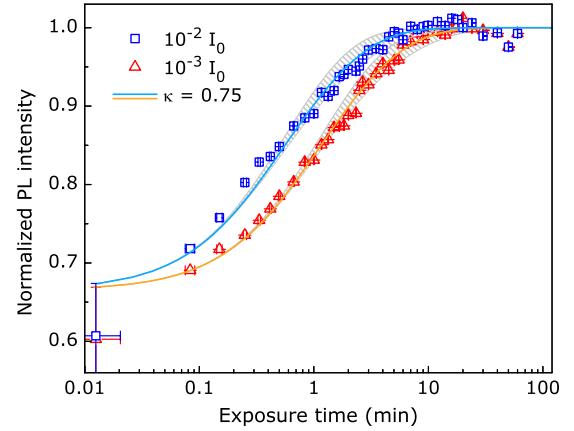


FIG. 3. (Color online) Evolution of the PL signal under continuous UV exposure for a second GaN NW sample. The experiments were performed at room temperature and for two different excitation densities. Both data sets are modeled with $\kappa=0.75$, the hatched area depicts the range of $0.5 < \kappa < 0.9$. The increased uncertainty of the first data point is due to the simultaneous beginning of the PL signal recording and UV exposure, introducing an error of about 10%. For the following data points, the vertical error bar, which is exclusively due to noise in the PL spectra, is given by the symbol size.

Since the PL signal is too weak at lower excitation whereas the initial increase of PL intensity is too fast at higher excitation, the range of excitation intensities is restricted to one order of magnitude.

The model presented above explains the temporal evolution of the NW PL intensity on a time scale of minutes. It does not, however, shed any light on the actual microscopic mechanism responsible for this change. For revealing this mechanism, we performed TRPL measurements while monitoring the desorption process. Although excitation and thus also desorption is pulsed in this case, the long-term temporal evolution of the integrated PL intensity is essentially identical.

The spectrally integrated transients after 8 s, 49 s, and 17 min of UV exposure are shown in Fig. 4(a). Irrespective of the exposure time, a clear biexponential behavior can be observed for which the long (short) component has a constant decay time τ_{eff} of approximately 140 ps (20 ps). Since the radiative lifetime τ_r in high-quality GaN exceeds 500 ps,^{22–24} the recombination process in our NWs must be dominated by nonradiative recombination, i.e., $\tau_{\text{eff}} \approx \tau_{\text{nr}}$.²⁵ TRPL studies of GaN NWs with different lengths indicate that the initial rapid decay is related to nonradiative recombination at the bottom of the NWs. The short component vanishes with increasing length. We thus neglect the initial rapid decay in the present analysis and consider only the slow decay at longer times of the transients.

Figure 4(b) depicts the individual transients of the (D^0, X) and (U, X) transitions after 17 min of UV exposure. It reveals clearly distinguishable nonradiative lifetimes $\tau_{D, \text{nr}}$ and $\tau_{U, \text{nr}}$ for the two transitions. Also, the temporal evolution of $\tau_{D, \text{nr}}$ and $\tau_{U, \text{nr}}$ differs. While the latter one remains constant at about 165 ps, $\tau_{D, \text{nr}}$ slightly increases from 60 to 100 ps [cf. Figure 4(c)]. Contrary to intuition, the desorption process

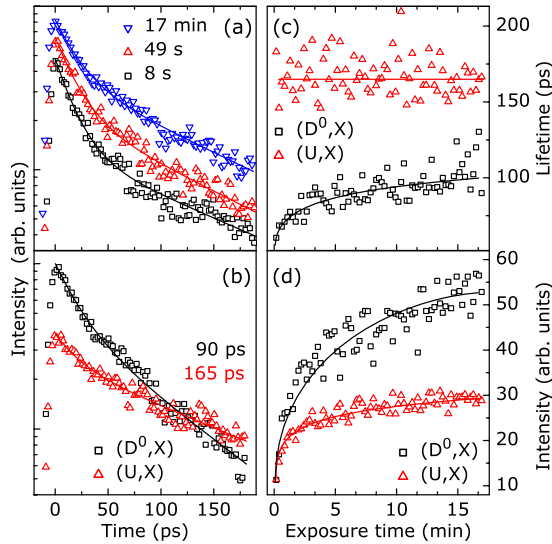


FIG. 4. (Color online) Evolution of the time-resolved PL signal under pulsed UV excitation at 10 K. (a) Spectrally integrated transients of the GaN NW ensemble for different exposure times as indicated. (b) Spectrally resolved transients for the (D^0, X) and (U, X) transition after 17 min of exposure. The lines in (a) and (b) are biexponential fits. In (b) $\tau_{D, nr}$ and $\tau_{U, nr}$ are given. (c) Evolution of the decay time of the (D^0, X) and (U, X) transition. (d) Evolution of the temporally integrated intensity of the (D^0, X) and (U, X) transition. The lines in (c) and (d) serve as a guide to the eyes.

thus does *not* reduce sufficiently the nonradiative surface recombination to account for the increase of intensity, which amounts for the (D^0, X) and (U, X) transitions to a factor of 4.7 and 2.4, respectively [see Fig. 4(d)]. Instead, the increase of the initial intensity [at $t=0$ in the transients shown in Fig. 4(a)] directly demonstrates a significant decrease of the *radiative* lifetime τ_r (for a general derivation of this relation, we refer the reader to the Appendix of Ref. 26). Specifically, the radiative lifetime $\tau_{D, r}$ ($\tau_{U, r}$) is reduced by a factor of 2.1 (2.4), yielding a corresponding enhancement of the quantum efficiency η . As we observe a change in the radiative lifetime, we can rule out that the increase of the PL intensity is induced by an enhanced exciton generation rate due to the altered surface, since the excitonic radiative lifetime does not depend on the generation rate.²⁷

Two important points have to be stressed in this context:

(i) Electrical measurements on NWs with exceptionally large diameters ($d=200$ nm) did not yield any detectable current indicating complete depletion. The alignment of the conduction and valence bands across the NW diameter can be obtained by solving the Poisson equation in cylindrical geometry.^{8,28} With $d=200$ nm and a Fermi level pinning of 0.6 eV below the conduction band edge,^{29,30} the threshold doping level above which the NW should be conductive is about $5 \times 10^{16} \text{ cm}^{-3}$. Since the investigated NWs have an average diameter of about 40 nm, they are certainly fully depleted (compare, for example, with the results of Calarco *et al.*²⁹). The band bending obtained from solving the Poisson equation translates into an electric field at the sidewall surface of these NWs of about 10 kV/cm. The comparison of

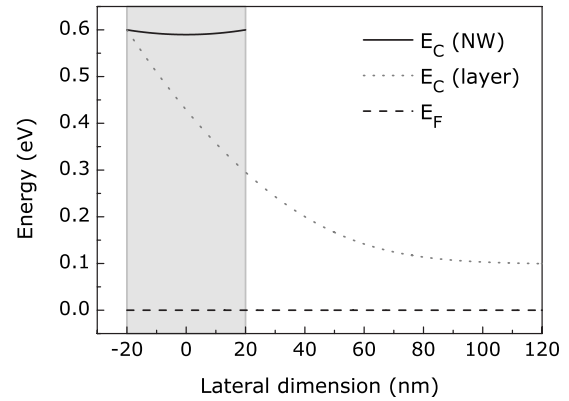


FIG. 5. Projection of the conduction band minimum in a NW with a diameter of 40 nm and a doping density of $5 \times 10^{16} \text{ cm}^{-3}$ (solid line). The dotted line depicts the conduction band at the surface of a layer with the same doping density. The gray area indicates the vertical NW cross section.

the conduction band profile in a GaN NW ($d=40$ nm) with the surface band profile in a GaN layer (Fig. 5) demonstrates that the surface electric field is drastically reduced in these thin, fully depleted NWs.

(ii) Electric fields of this magnitude lead to a quenching of the exciton luminescence, but not to a spectral shift.^{31,32} The quenching is caused by the field or impact ionization of the exciton, leading to a drop of the radiative recombination efficiency. The transfer of positive charges to the surface²¹ upon UV exposure reduces the electric field and thus increases the recombination efficiency, while it does not affect the peak position.³² Another mechanism reducing the field would be screening. However, in order to reduce the field *in the course* of the measurement, an increase of the carrier density would be required. As we keep the excitation intensity constant throughout the measurement, we can exclude screening as a possible origin for the field reduction.

In order to draw the main conclusion, let us summarize our most important findings at this point. First, oxygen desorption results in an increase of the *radiative recombination rate*. Second, the transition energy stays *perfectly constant* throughout the desorption process. The only possible mechanism that is consistent with both facts is the presence of an electric field within the NW slowing down exciton recombination and a *subsequent* reduction of this field upon oxygen desorption. Since the surface electric field strength is entirely determined by the Fermi level pinning and the doping of the NW (which is not changed upon oxygen desorption), a reduction of the field strength inevitably implies an unpinning of the Fermi level.

Finally, Corfdir *et al.*¹⁷ have ascribed the (U, X) transition to originate from a TES of the (D^0, X) located in the vicinity of the NW surface. In other words, they interpret the (U, X) line to stem mostly from a region close to the NW surface, whereas they believe the (D^0, X) luminescence to originate mainly from the bulklike inner part of the NW. If this interpretation was correct, both the (D^0, X) and the (U, X) transition should to first order display an identical PL intensity increase with decreasing electric fields.³³ Experimentally, however, the (U, X) PL exhibits a much less pronounced in-

tensity increase compared to that of the (D^0, X) transition, implying that the binding energy of the excitonic complex is significantly higher as also reflected by the energy of this transition.³²

To summarize and conclude, we have shown that the exposure of GaN NWs to ultraviolet radiation induces desorption of oxygen from the NW sidewalls, which in turn results in an unpinning of the Fermi level at the surface. The corresponding reduction of the electric fields in the NWs leads to an enhanced radiative decay rate of bound excitons and to an increase of the PL intensity by as much as a factor of 2 to 5. These findings underline the importance of electric fields in NWs. Note that, for low doping densities such as present in the active region of light emitters, no field-free region exists within the NW. This fact most explicitly emphasizes the im-

portance of surface passivation for the application of GaN NWs in future devices. We furthermore established a random-walk model describing the desorption process in NW ensembles on a macroscopic time scale. The simulations show that readsorption of oxygen on adjacent NWs delays the overall desorption process significantly.

The authors wish to thank Y. Takagaki for the conductance measurements. We furthermore thank C. G. Van de Walle for inspiring discussions and L. Schrottke for a critical reading of the paper. This work was partially supported by the EU Marie Curie RTN Contract No. MRTN-CT-2004-005583 (PARSEM), by the IST project NODE Grant No. 015783, and by the German BMBF joint research project MONALISA (Contract No. 01BL0810).

*pfueller@pdi-berlin.de

- ¹M. G. Lagally and R. H. Blick, *Nature (London)* **432**, 450 (2004).
- ²C. M. Lieber and Z. L. Wang, *MRS Bull.* **32**, 99 (2007).
- ³J. A. Czaban, D. A. Thompson, and R. R. LaPierre, *Nano Lett.* **9**, 148 (2009).
- ⁴J. B. Schlager, K. A. Bertness, P. T. Blanchard, L. H. Robins, A. Roshko, and N. A. Sanford, *J. Appl. Phys.* **103**, 124309 (2008).
- ⁵O. Brandt, C. Pfüller, C. Chèze, L. Geelhaar, and H. Riechert, *Phys. Rev. B* **81**, 045302 (2010).
- ⁶G. M. Dalpian and J. R. Chelikowsky, *Phys. Rev. Lett.* **96**, 226802 (2006).
- ⁷M. V. Fernández-Serra, C. Adessi, and X. Blase, *Phys. Rev. Lett.* **96**, 166805 (2006).
- ⁸B. S. Simpkins, M. A. Mastro, J. C. R. Eddy, and P. E. Pehrsson, *J. Appl. Phys.* **103**, 104313 (2008).
- ⁹E. Calleja, M. A. Sánchez-García, F. J. Sánchez, F. Calle, F. B. Naranjo, E. Muñoz, U. Jahn, and K. Ploog, *Phys. Rev. B* **62**, 16826 (2000).
- ¹⁰R. Meijers, T. Richter, R. Calarco, T. Stoica, H. P. Bochem, M. Marso, and H. Lüth, *J. Cryst. Growth* **289**, 381 (2006).
- ¹¹O. Brandt, T. Fliesskowski, D. M. Schaadt, U. Jahn, A. Trampert, and H. T. Grahn, *Appl. Phys. Lett.* **93**, 081907 (2008).
- ¹²A. Wyszomolka, K. P. Korona, R. Stępniewski, J. M. Baranowski, J. Błoniarz, M. Potemski, R. L. Jones, D. C. Look, J. Kuhl, S. S. Park, and S. K. Lee, *Phys. Rev. B* **66**, 245317 (2002).
- ¹³K. Kornitzer, T. Ebner, M. Grehl, K. Thonke, R. Sauer, C. Kirchner, V. Schwegler, M. Kamp, M. Leszczynski, I. Grzegory, and S. Porowski, *Phys. Status Solidi B* **216**, 5 (1999).
- ¹⁴P. P. Paskov, T. Paskova, P. O. Holtz, and B. Monemar, *Phys. Rev. B* **70**, 035210 (2004).
- ¹⁵F. Furtmayr, M. Vielmeyer, M. Stutzmann, A. Laufer, B. K. Meyer, and M. Eickhoff, *J. Appl. Phys.* **104**, 074309 (2008).
- ¹⁶L. H. Robins, K. A. Bertness, J. M. Barker, N. A. Sanford, and J. B. Schlager, *J. Appl. Phys.* **101**, 113505 (2007).
- ¹⁷P. Corfdir, P. Lefebvre, J. Ristić, P. Valvin, E. Calleja, A. Trampert, J.-D. Ganière, and B. Deveaud-Plédran, *J. Appl. Phys.* **105**, 013113 (2009).
- ¹⁸V. Consonni, M. Knelangen, U. Jahn, A. Trampert, L. Geelhaar, and H. Riechert, *Appl. Phys. Lett.* **95**, 241910 (2009).
- ¹⁹U. Behn, A. Thamm, O. Brandt, and H. T. Grahn, *J. Appl. Phys.* **87**, 4315 (2000).
- ²⁰M. Foussekis, A. A. Baski, and M. A. Reshchikov, *Appl. Phys. Lett.* **94**, 162116 (2009).
- ²¹S. R. Morrison, *The Chemical Physics of Surfaces*, 1st ed. (Plenum Press, New York, 1977) (and references therein).
- ²²G. E. Bunea, W. D. Herzog, M. S. Ünlü, B. B. Goldberg, and R. J. Molnar, *Appl. Phys. Lett.* **75**, 838 (1999).
- ²³B. Monemar, P. P. Paskov, J. P. Bergman, A. A. Toropov, T. V. Shubina, T. Malinauskas, and A. Usui, *Phys. Status Solidi B* **245**, 1723 (2008).
- ²⁴U. Özgür, Y. Fu, Y. T. Moon, F. Yun, H. Morkoç, H. O. Everitt, S. S. Park, and K. Y. Lee, *Appl. Phys. Lett.* **86**, 232106 (2005).
- ²⁵The effective lifetime τ_{eff} is given by $\tau_{\text{eff}}^{-1} = \tau_{\text{nr}}^{-1} + \tau_{\text{r}}^{-1}$, whereas the quantum efficiency η can be written as $\eta = \tau_{\text{eff}} / \tau_{\text{r}}$.
- ²⁶O. Brandt, P. Waltereit, S. Dhar, U. Jahn, Y. Sun, A. Trampert, K. Ploog, M. Tagliente, and L. Tapfer, *J. Vac. Sci. Technol. B* **20**, 1626 (2002).
- ²⁷O. Brandt, K. Kanamoto, M. Gotoda, T. Isu, and N. Tsukada, *Phys. Rev. B* **51**, 7029 (1995).
- ²⁸G. L. Snider, I.-H. Tan, and E. L. Hu, *J. Appl. Phys.* **68**, 2849 (1990).
- ²⁹R. Calarco, M. Marso, T. Richter, A. Aykanat, R. Meijers, A. d. Hart, T. Stoica, and H. Lüth, *Nano Lett.* **5**, 981 (2005).
- ³⁰C. G. Van de Walle and D. Segev, *J. Appl. Phys.* **101**, 081704 (2007).
- ³¹J. Camacho, P. Santos, F. Alsina, M. Ramsteiner, K. Ploog, A. Cantarero, H. Obloh, and J. Wagner, *J. Appl. Phys.* **94**, 1892 (2003).
- ³²J. Pedrós, Y. Takagaki, T. Ive, M. Ramsteiner, O. Brandt, U. Jahn, K. H. Ploog, and F. Calle, *Phys. Rev. B* **75**, 115305 (2007).
- ³³According to this interpretation, the (U,X) experiences an even stronger electric field than the (D^0, X) due to the surface band bending. Furthermore, surface donors exhibit a lower exciton binding energy than bulklike donors (Ref. 5). Both of these facts should to second order even result in a stronger increase for the (U,X) line compared to the (D^0, X) transition (Ref. 32) contrary to what is observed experimentally.